

Article

High-Efficiency and Low-Damage Lapping Process Optimization

Ci Song * , Feng Shi, Wanli Zhang, Zhifan Lin and Yuxuan Lin

Laboratory of Science and Technology on Integrated Logistics Support, College of Intelligence Science and Technology, National University of Defense Technology, Changsha 410073, China; shifeng@nudt.edu.cn (F.S.); linzhifan16@nudt.edu.cn (Z.L.); zhangwanli17@nudt.edu.cn (W.Z.); zhongdayuu@gmail.com (Y.L.)

* Correspondence: songci@nudt.edu.cn

Received: 4 December 2019; Accepted: 20 January 2020; Published: 24 January 2020



Abstract: The silica optics are widely applied in the modern laser system, and its fabrication is always the research focus. In the manufacturing process, the lapping process occurs between grinding and final polishing. However, lapping processes optimizations focus on decreasing the depth of sub-surface damage (SSD) or improving lapping efficiency individually. So, the optimum balance point between efficiency and damage should be studied further. This manuscript establishes the effective removal rate of damage (ERRD) model, and the relationship between the ERRD and processing parameters is simulated. Then, high-efficiency, low-damage lapping processing routine is established based on the simulation. The correctness and feasibility are validated. In this work, the optimized method is confirmed that it can improve efficiency and decrease damage layer depth in the lapping process which promotes the development of optics in low-damage fabrication.

Keywords: low-damage fabrication; effective removal rate of damage; lapping process; sub-surface damage

1. Introduction

Fused silica optics with excellent surface and sub-surface quality are widely used in high power laser system [1]. For example, the system of National Ignition Facility (NIF) contains thousands of fused silica optics that precisely guide, reflect, amplify, and focus 192 laser beams onto a fusion target [2]. However, the laser induced-damage initiation on fused silica optics limits the performance of high-power laser applications [3]. In the previous study, some researchers have shown that sub-surface damage (SSD) is likely to be laser damage precursors [4]. It can cause laser damage susceptibility regionally, enhance laser absorption, and then introduce macroscopic damage to optics [5,6]. In order to avoid degradation of quality, SSD must be minimized or eliminated in the fabrication of optics.

The optical fabrication process mainly contains grinding, lapping and polishing. SSD is introduced in the grinding process and restrained in the following process [7–9]. Figure 1 illustrates the generation of SSD during manufacturing. To remove SSD in grinding processing, it needs to remove materials to 3~9 times of grinding abrasive size in the lapping process, which is time-consuming and inefficient [10]. For the lapping process, the material removal occurs into two types: brittle domain and plastic domain. The division of material removal domain is related to an external load and the properties of the material itself. In the brittle domain, cracks appear on the surface and materials are sheared off from substrate under the load, which can achieve higher material removal efficiency. Differently, materials are removed through the function of plastic flow in the plastic domain whose removal is relatively inefficient. In the previous study, a high-efficiency lapping process tends to increase the depth of SSD and delay the processing cycle since the material removal rate of final polishing is rather low. On the

other hand, if processing efficiency is reduced to control SSD, more time would be consumed [11]. The main problem is that efficiency and SSD controlling are not balanced in the lapping process.

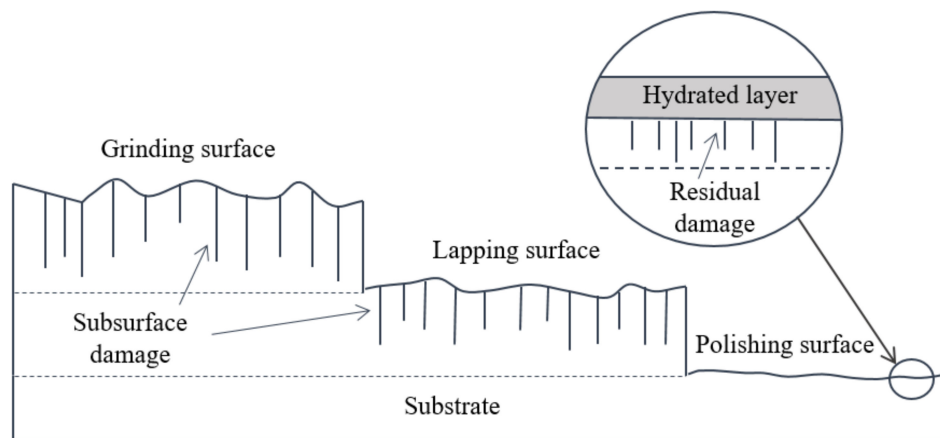


Figure 1. The schematic view of sub-surface damage (SSD) from grinding to polishing.

Buijs et al. had found that the energy required for material fracture removal was lower than that for plastic deformation, and the critical load of median cracks of fused silica was 0.02N through Vickers indentation experiment. A model was also established to predict removal efficiency [12]. Lambropoulos et al. had proposed an interpretation of manufacturing features based on the optical material removal micromechanical model, which could conduct the fabrication process [13]. More recently, Neauport et al. studied the effect of lapping parameters with different lapping slurries on roughness and SSD. After lapping under the optimal parameters (abrasive: Al_2O_3 , grain size: 3 μm , lapping speed: 50 rpm, load: 2.8 kg), the roughness R_t of fused silica is 1.3 μm and SSD depth is 4.3 μm , while material removal rate was relatively small [14]. From above all the researches, they focused on decreasing the depth of SSD or improving lapping efficiency individually.

To optimize the lapping process, a theoretical model is proposed and optimal lapping parameters are applied in the manufacture of optics. This work is organized as follows: Section 1 is Introduction. Section 2 presents the model and basic equation, which describes the establishment of the remove rate model, subsurface defect model and the effective removal rate of damage (ERRD) model in detail. Section 3 is the simulation while Section 4 is the experimental validation. Section 5 is the conclusion of the work. In general, the theoretical model and the optimal lapping parameters can be a reference on high-efficiency, low-damage optics fabrication.

2. Model and Basic Equation

2.1. Remove Rate Model and Subsurface Defect Model

In reality, as shown in Figure 2, the material is often removed by a combination of various mechanical mechanisms [15]. This co-existence of mechanisms is believed to be caused by non-uniform depth of penetrations among abrasives. Usually, abrasives with large sizes would embed in both the workpiece surface and lapping plate, bear the load, and then remove the materials from the workpiece along with the motion of the lapping plate. Conversely, abrasives with small size adhere to the surface, which can not achieve effective material removal. It should be noted that cracks appeared along with material removal (brittle domain) when an external load is large enough. Meanwhile, smaller hardness of lapping plate or workpiece would promote the function of rolling of abrasives and finally achieves three-body machining. Considering the hardness of iron lapping plate and external load, the model focuses on three-body and brittle machining [11].

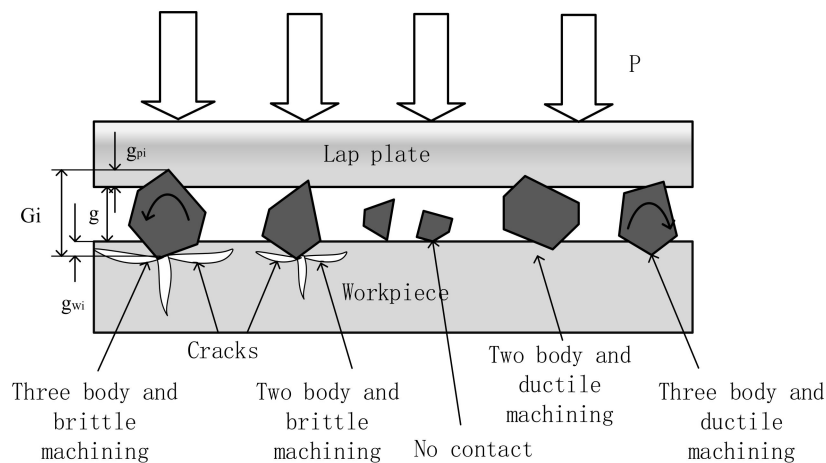


Figure 2. Interaction among abrasive, lapping plate and workpiece.

In the three-body and brittle lapping process, the force borne by the single abrasive can be defined as in Equation (1) [15,16].

$$F_i = \alpha \cdot (x - g)^2 / \left(1 / \sqrt{H_w} + 1 / \sqrt{H_p}\right)^2, \tag{1}$$

where α is geometric constant depends on the abrasive shape, it can be calculated as $\alpha = 4 \cdot \tan^2 \psi$, ψ is the sharpness angle of abrasive; x is the size of abrasive; g is the gap between workpiece and lapping plate; H_w is the hardness of workpiece; H_p is the hardness of lapping plate.

The total load F can be expressed as Equation (2).

$$\left\{ \begin{aligned} F &= \sum_{x_i > g} F_i = N \int_g^{x_{\max}} [F(x) \cdot \varphi(x)] dx = \frac{\alpha \cdot N}{(1 / \sqrt{H_w} + 1 / \sqrt{H_p})^2} \cdot \int_g^{x_{\max}} [(x - g)^2 \cdot \varphi(x)] dx \dots\dots 1 \\ \varphi(x) &= \frac{f(x)}{\int_{x_{\min}}^{x_{\max}} f(x) dx} = \frac{e^{\frac{1}{2} \frac{\ln(x-a_1)a_2^2}{a_3}}}{\sqrt{2}(x-a_1)a_3 \int_{x_{\min}}^{x_{\max}} f(x) dx} \dots\dots 2 \end{aligned} \right. , \tag{2}$$

where $\varphi(x)$ is bounded lognormal distribution; N is the total number of abrasive, it can be calculated by Equation (3) [17].

$$\left\{ \begin{aligned} N &= \frac{A \cdot x_{\max}}{V \cdot (1 + \frac{\rho_a}{m \rho_l})} \dots\dots 1 \\ V &= \frac{\pi \cdot (x_{\text{avg}})^3}{6} \dots\dots 2 \end{aligned} \right. , \tag{3}$$

where A is the contact area between lapping plate and workpiece; ρ_a and ρ_l is the density of abrasive particles and lapping slurry respectively; m is the weight ratio of abrasive particles in lapping slurry.

Some researchers have derived theoretical equations of median crack depth and lateral crack depth, based on indentation of sharp indenter [18]. Figure 3 illustrates the crack systems under indentation.

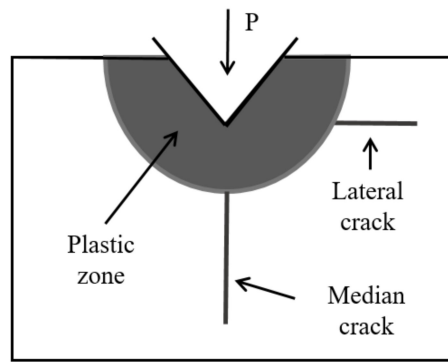


Figure 3. Micro-indentation mechanics.

According to previous study, the depth of SSD is equal to that of median crack Cm , and it can be written as Equation (4).

$$Cm = \alpha_K^{2/3} \cdot \left(\frac{E_w}{H_w}\right)^{(1-m)2/3} \cdot (\cot \psi)^{4/9} \cdot \left(\frac{F}{K}\right)^{2/3}, \tag{4}$$

where E_w is the elastic modulus; H_w is the hardness of material; α_k is a dimensionless constant, which can be defined as $\alpha_k = 0.027 + 0.090(m-1/3)$, the value of m is 0.5; F is the load that lapping plate exerts; K is the dynamic fracture toughness related to the properties of materials.

The lateral crack is related to the removal rate, the length CL can be defined as Equation (5).

$$CL = \left(\frac{\xi}{M}\right)^{1/2} \cdot (\cot \psi)^{5/12} \cdot \frac{E_w^{3/8}}{K^{1/2} H_w^{1/2}} \cdot F^{5/8} \tag{5}$$

where ξ is a constant which can be obtained through experiment; M is a geometrical constant, $M = 0.75$.

The material removal rate (MRR) can be expressed as Equation (6).

$$\left\{ \begin{array}{l} MRR = n \frac{dv}{dt} \dots\dots 1) \\ \frac{dv}{dt} = \pi (CL)^2 \cdot (Cm) \cdot \frac{2V}{\pi s_{avg}} \dots\dots 2) \\ s_{avg} = \frac{\int_d^{x_{max}} x \varphi(x) dx}{\int_d^{x_{max}} \varphi(x) dx} \dots\dots 3) \end{array} \right. , \tag{6}$$

where V is abrasive velocity; n is the effective number of abrasive, which can be written as:

$$n = N \int_g^{x_{max}} \varphi(x) dx. \tag{7}$$

2.2. ERRD Model

The optimization of efficiency and SSD are two important targets in the lapping process. However, they cannot be achieved at the same time, because of lacking in theoretical analysis. To quantify the efficiency and SSD, the ERRD model is proposed. It can be expressed as follows:

$$ERRD = \frac{SSD_{before} - SSD_{after}}{t} \tag{8}$$

$$t = \frac{H \times S_{workpiece}}{MRR} \quad (9)$$

$$ERRD = \frac{(SSD_{before} - SSD_{after}) \times MRR}{H \times S_{workpiece}}, \quad (10)$$

where K is ERRD, its unit is $\mu\text{m}/\text{min}$; H is removal depth in lapping process, its unit is μm ; t is processing time, its unit is min ; S is the area of surface, its unit is mm^2 ; MRR is the volume removal efficiency in lapping process, its unit is $\mu\text{m}^3/\text{min}$.

It should be noted that SSD represents the length of the median crack. In order to simplify the calculation, we use the damage depth to replace it, and its unit is μm .

The ERRD model can be used to find the balance point between SSD and removal efficiency. According to Equations (8) and (9), the value of ERRD is positively related to material removal rate under the same condition of SSD . Moreover, it shows negative correlation between ERRD and removal rate under the same condition of removal efficiency, according to Equation (10). The optimization of SSD and removal efficiency could refer to the ERRD model.

3. Simulations

The factors affecting removal efficiency and SSD in the lapping process mainly include abrasive, pressure and lapping velocity [19]. To optimize efficiency and control the depth of SSD , the relationship between ERRD and these factors were analyzed.

(1) Abrasive

The type and particle size are two key factors that affect the efficiency and depth of SSD [20]. In this work, different abrasive types and particle sizes are chosen to simulate.

The processing parameters are set as: 40 mm lapping tool size, 0.1 MPa lapping pressure, and 120 rpm lapping velocity. The relationship between ERRD and abrasive can be obtained from simulation, as shown in Figure 4.

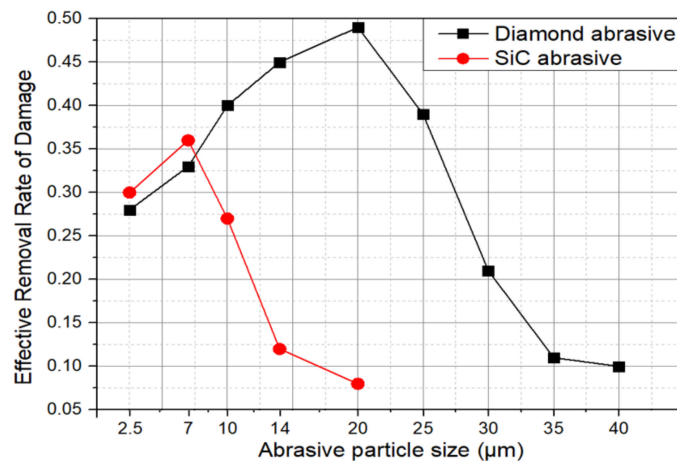


Figure 4. The relationship between effective removal rate of damage (ERRD) and abrasive.

Based on the results, it can be concluded that: (1) ERRD value of diamond abrasive is 1.5~3 times of silicon carbide (SiC) with the same particle size, except for W2.5 and W7. (2) Both curves of ERRD increase firstly and then reduce. (3) The largest ERRD value of silicon carbide (SiC) achieves when particle size is W7 (7 μm), while that of diamond is W20 (20 μm).

(2) Pressure

The processing parameters are set as: 40 mm lapping tool size, silicon carbide abrasive, W10 abrasive, and 180 rpm lapping velocity. The relationship between ERRD and lapping pressure can be obtained from the results, as shown in Figure 5. It can be seen ERRD is linear with lapping pressure, which means that large pressure tends to improve ERRD under the conditions of stable process parameters.

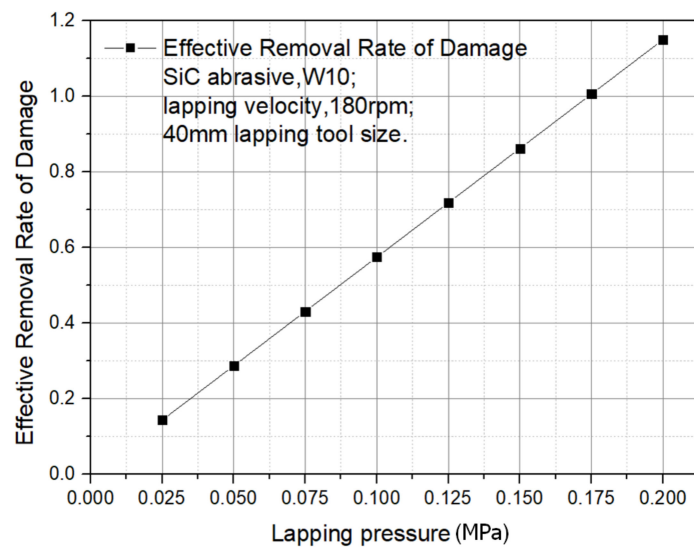


Figure 5. ERRD for various lapping pressure.

(3) Velocity

The process parameters are 40 mm lapping tool size, silicon carbide abrasive, W10 abrasive, and 0.2 MPa lapping pressure.

The relationship between the ERRD and lapping velocity can be obtained from Figure 6. According to the result, ERRD is nonlinear with lapping velocity. When lapping velocity beyond 90 rpm, the value of ERRD grows faster.

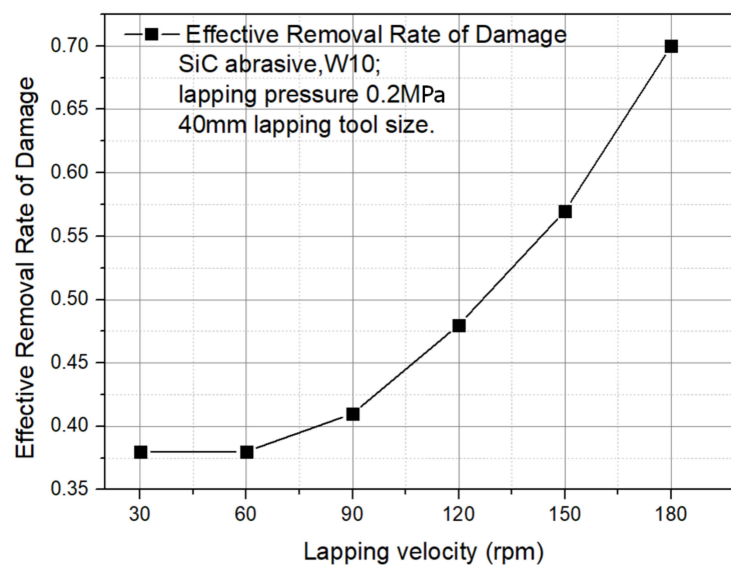
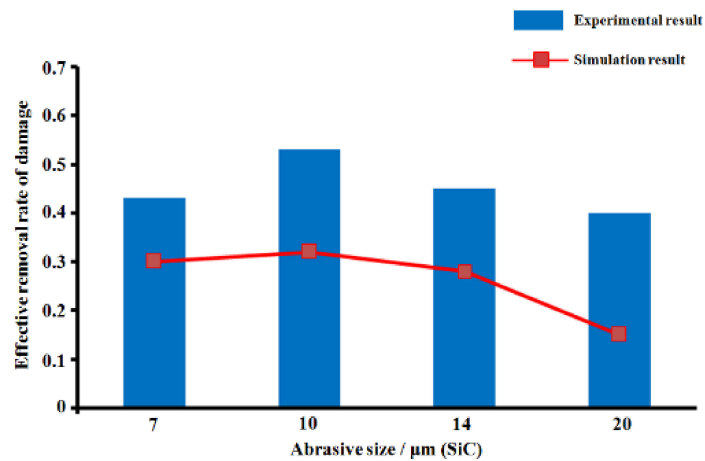


Figure 6. ERRD for different lapping velocity.

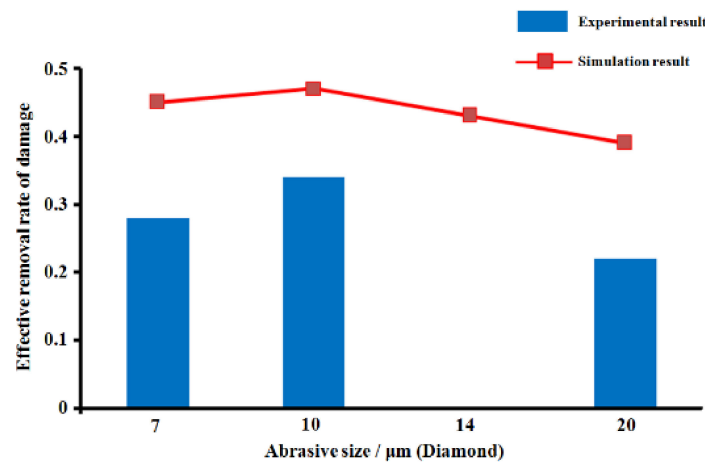
4. Experimental Validation

(1) Validation of simulation parameters

After the ERRD model is established, we carried out a verification experiment to verify the accuracy of the model. In the verification experiment, abrasives with different particle sizes were used as verified objects. Corining 7980 fused silica samples (size: 10 mm × 10 mm, number: 7) were used as the materials, concentration of lapping slurry is 5%, lapping velocity is 120 rpm, 0.2 MPa lapping pressure, and 200 μm material removal depth. The results are shown in Figure 7.



(a) Result of SiC abrasive with different particle sizes.



(b) Result of diamond abrasive with different particle sizes.

Figure 7. Results of ERRD with different abrasive.

According to the results shown in Figure 7, ERRD (effective removal rate of damage) of SiC abrasive was higher than that of diamond abrasive under the same conditions. In Figure 7a, the values of simulation results were lower than experimental results, which were contrary to the results shown in Figure 7b. For Figure 7a, the highest ERRD occurred when 10 μm SiC abrasives were used, and its value was 0.53 μm/min. For Figure 7b, the highest ERRD value was 0.34 μm/min, while the diamond abrasive size 10 μm. Though the experiment results were different from the simulation, their trends were the same. In consideration of ERRD, 10 μm SiC abrasives can be applied in the lapping process. (14 μm diamond abrasive is not applied in the experiment because of the limitation of resource in our team). Afterwards, the lapping velocity is regarded as the object and the result is shown in Figure 8.

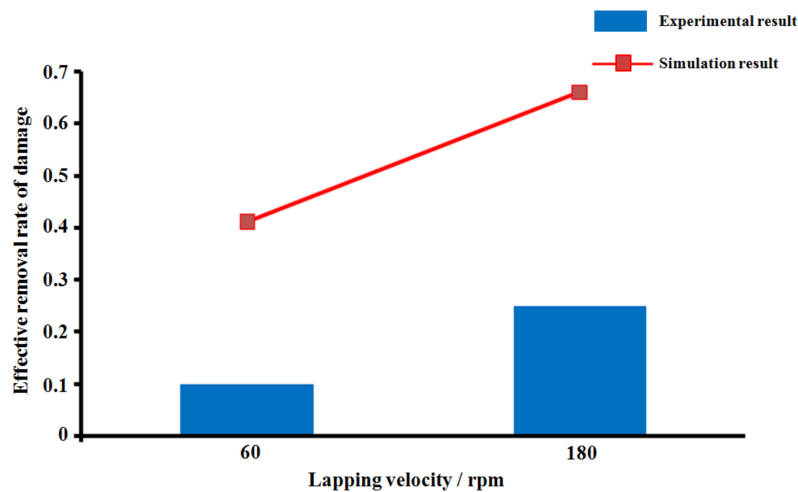


Figure 8. Result of ERRD under different lapping velocity.

In Figure 8, the trend of experimental results is the same as that of simulation results. According to Equation (10), a higher material removal rate (MRR) would improve the value of ERRD. Limited by the performance of the machine tool, the lapping velocity can be set at 180 rpm. It should be noted that the processing environment, conditions of lapping slurry and other factors may influence experimental results.

(2) Validation of rough and fine lapping process.

The simulation in Sections 3 and 4.(1) provides references to optimize lapping parameters. In the actual lapping process, lapping pressure needs to be controlled strictly. Excessive pressure would push the lapping slurry out of the lapping area and make direct contact between the lapping plate and the surface [21]. Limited by machine tool, the velocity is not more than 180 rpm. According to Figure 4, W20 diamond abrasive and W7 SiC abrasive are utilized in the experiment. The parameters are all listed in Table 1. The total material removal amount in Process A and Process B are the same as the conventional lapping process.

Table 1. Process parameters in the lapping process.

Item	Conventional Lapping	Process A	Process B
Material removal amount	250 μm	250 μm	250 μm
Abrasive	SiC	Diamond	SiC
Abrasive size	W20	W20	W7
Pressure	0.2 MPa	0.2 MPa	0.2 MPa
Velocity	120 rpm	180 rpm	180 rpm

Three Corning 7980 fused silica samples with 100 mm \times 100 mm (sample 1–4) were prepared on a single side polishing machine. Sample 1 was lapped by the conventional process. Sample 2 and sample 3 were lapped by processes A and B, respectively. Sample 4 was lapped by a rough and fine lapping process. Then, four samples were polished by the MRF wedge method, and the damage depth was measured by the microscope.

As shown in Figure 9, cracks existed on the initial surface, and their amount reduces when the polishing depth increases. The cracks almost disappear when the polishing depth increases to 18.76 μm . Therefore, the damage depth of sample 1 should be 18.76 μm .

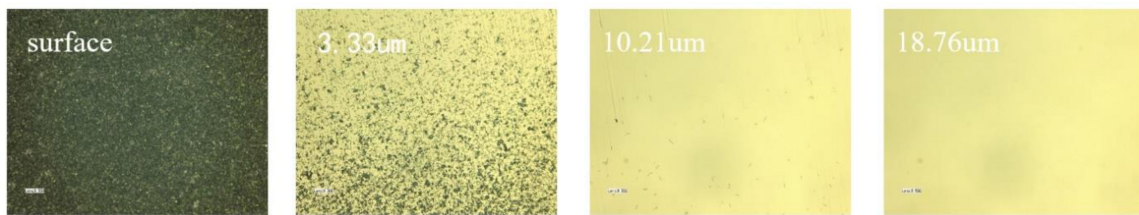


Figure 9. SSD results of sample 1.

The results of sample 2 show that cracks reduce when depth increases, see Figure 10. However, it still exists at the depth of 26.88 μm where cracks already disappear on sample 1. Therefore, we keep on lapping, and the cracks disappear at the depth of 40.14 μm. As shown in Figure 11, it can be clearly seen that the damage depth of sample 3 is 6.83 μm. Compared with the conventional lapping process, process B can significantly decrease the depth of SSD.

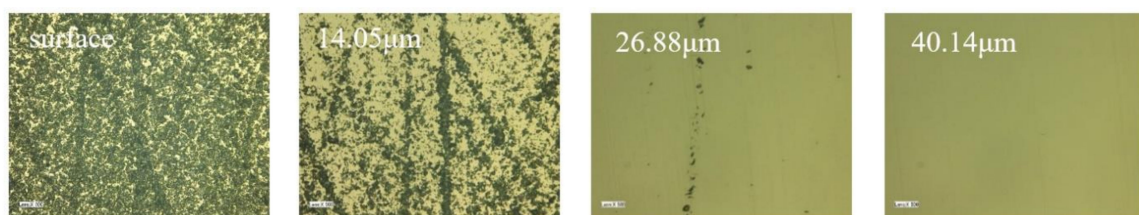


Figure 10. SSD results of sample 2.

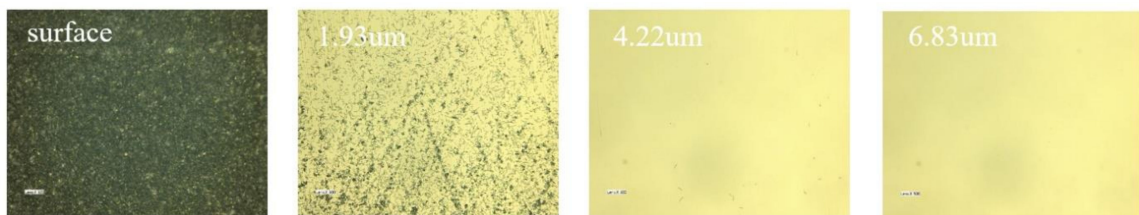


Figure 11. SSD results of sample 3.

The detailed results listed in Table 2 are to evaluate the effect under different lapping parameters. We can find that the efficiency of process A is the highest among the three processes, while the SSD depth of process B is the shallowest.

Table 2. Results under different lapping parameters.

Item	Conventional Process	Process A	Process B
Lapping Time (h)	9	2.5	5.3
SSD depth (μm)	18.76	40.14	6.83

As shown in Table 3, we choose W20 diamond and W7 SiC as the rough lapping abrasive and fine lapping abrasive, respectively. The removal amount is 200 μm in rough lapping and 50 μm in fine lapping. The lapping pressure is 0.2 MPa and velocity is 180 rpm. Total lapping time is 3.1 h (2h rough lapping and 1.1 h fine lapping) and the lapping results are shown in Figure 12.

Table 3. Parameter of optimum lapping process.

Item	Rough Lapping	Fine Lapping
Material removal amount	200 μm	50 μm
Abrasive	W20 Diamond	W7 SiC
Pressure	0.2 MPa	0.2 MPa
Velocity	180 rpm	180 rpm



Figure 12. SSD results of sample 4.

In Figure 12, the SSD depth of the sample is $6.11\ \mu\text{m}$ after the lapping process. Compared with the conventional lapping process, the combination of rough and fine lapping processes was more efficient, which reduced lapping time by 65% with the same material removal ($250\ \mu\text{m}$). Meanwhile, the SSD depth reduces from $18.76\ \mu\text{m}$ to $6.11\ \mu\text{m}$. The results demonstrated that rough and fine lapping can not only reduce SSD depth but also improve the removal efficiency.

5. Conclusions

In this work, the ERRD model is established to provide a theoretical reference about balancing lapping efficiency and SSD, the relationship between ERRD, abrasive type, abrasive size, pressure and velocity is simulated. Through the simulation, W7 SiC abrasive and W20 diamond abrasive can be applied in the lapping process, while lapping pressure needs to be controlled strictly. Limited by the performance of the machine tool, the lapping velocity is set at 180 rpm. Based on the simulation, the validation experiments are carried out. In the experiment, the optimal parameters are applied to rough lapping and fine lapping process. After lapping, the depth of SSD decreases from $18.76\ \mu\text{m}$ to $6.11\ \mu\text{m}$ and processing time decreased from 9 h to 3.1 h, reduces by 65% compared with conventional parameters. The results indicate that the optimum lapping process can not only improve efficiency but also reduce SSD depth. Therefore, the ERRD model and optimum lapping process can be applied in high-efficiency, low-damage lapping process optimization for high power laser optics.

Author Contributions: Conceptualization, F.S.; investigation, W.Z., Y.L.; methodology, C.S.; supervision, C.S.; validation, F.S.; visualization, Z.L.; writing—original draft, C.S.; Writing—review and editing, F.S. All authors have read and agreed to the published version of the manuscript.

Funding: This research was funded by the National Nature Science Foundation of China (NSFC) (No.51835013, No. 51675526, No.51775551).

Acknowledgments: Special thanks to scientists of the Hunan Key Laboratory of Ultra-Precision Machining Technology, Hunan, China, for their support and technical assistance.

Conflicts of Interest: The authors declare no conflict of interest.

References

1. Menapace, J.; Penetrante, B.; Miller, P.; Parham, T.; Nichols, M.; Peterson, J.; Golini, D. Combined advanced finishing and UV-laser conditioning for producing UV-damage-resistant fused silica optics. In *Optical Fabrication and Testing*; Optical Society of America: Washington, DC, USA, 2002.
2. Campbell, J.H.; Hawley-Fedder, R.A.; Stolz, C.J.; Menapace, J.A.; Borden, M.R.; Whitman, P.K.; Yu, J.; Runkel, M.J.; Riley, M.O.; Feit, M.D.; et al. NIF optical materials and fabrication technologies: an overview. In *Optical Engineering at the Lawrence Livermore National Laboratory II: The National Ignition Facility: International Society for Optics and Photonics*; International Society for Optics and Photonics: Washington, DC, USA, 2004; pp. 84–101.
3. Neauport, J.; Ambard, C.; Bercegol, H.; Cahuc, O.; Champreux, J.P.; Charles, J.L.; Cormont, P.; Darbois, N.; Darnis, P.; Destribats, J.; et al. Optimizing fused silica polishing processes for 351nm high-power laser application. In *Laser-Induced Damage in Optical Materials*; International Society for Optics and Photonics: Washington, DC, USA, 2008.

4. Huang, J.; Zhou, X.; Liu, H.; Wang, F.; Jiang, X.; Wu, W.; Tang, Y.; Zheng, W. Influence of subsurface defects on damage performance of fused silica in ultraviolet laser. *Opt. Eng.* **2013**, *52*, 52024203. [[CrossRef](#)]
5. Bloembergen, N. Role of cracks, pores, and absorbing inclusions on laser induced damage threshold at surfaces of transparent dielectrics. *Appl. Opt.* **1973**, *12*, 661–664. [[CrossRef](#)] [[PubMed](#)]
6. Genin, F.Y.; Salleo, A.; Pistor, T.V.; Chase, L.L. Role of light intensification by cracks in optical breakdown on surfaces. *JOSA A* **2001**, *18*, 2607–2616. [[CrossRef](#)] [[PubMed](#)]
7. Wang, Z.; Wu, Y.; Dai, Y.; Li, S. Subsurface damage distribution in the lapping process. *Appl. Opt.* **2008**, *47*, 1417–1426. [[CrossRef](#)] [[PubMed](#)]
8. Suratwala, T.; Wong, L.; Miller, P.; Feit, M.D.; Menapace, J.; Steele, R.; Davis, P.; Walmer, D. Sub-surface mechanical damage distributions during grinding of fused silica. *J. Non Cryst. Solids* **2006**, *352*, 5601–5617. [[CrossRef](#)]
9. Neauport, J.; Ambard, C.; Cormont, P.; Darbois, N.; Destribats, J.; Luitot, C.; Rondeau, O. Subsurface damage measurement of ground fused silica parts by HF etching techniques. *Opt. Express* **2009**, *17*, 20448–20456. [[CrossRef](#)] [[PubMed](#)]
10. Lee, Y. Evaluating subsurface damage in optical glasses. *J. Eur. Opt. Soc. Rapid Publ.* **2011**, *6*. [[CrossRef](#)]
11. Lin, Y.X.; Song, C.; Shi, F.; Li, S.Y. Modeling and simulation for effective removal rate of damage. In *Pacific Rim Laser Damage 2017: Optical Materials for High-Power Lasers*; International Society for Optics and Photonics: Washington, DC, USA, 2017; p. 103392B.
12. Buijs, M.; Korpel-van Houten, K. Three-body abrasion of brittle materials as studied by lapping. *Wear* **1993**, *166*, 237–245. [[CrossRef](#)]
13. Lambropoulos, J.C. Polishing rate of fused silica, compared to glasses BK7 and SF6. In *Optifab 2003: Technical Digest*; International Society for Optics and Photonics: Washington, DC, USA, 2003; p. 103140Q.
14. Neauport, J.; Destribats, J.; Maunier, C.; Ambard, C.; Cormont, P.; Pintault, B.; Rondeau, O. Loose abrasive slurries for optical glass lapping. *Appl. Opt.* **2010**, *49*, 5736–5745. [[CrossRef](#)] [[PubMed](#)]
15. Chang, Y.P.; Hashimura, M.; Dornfeld, D. An Investigation of Material Removal Mechanisms in Lapping with Grain Size Transition. *J. Manuf. Sci. Eng.* **2000**, *122*, 419. [[CrossRef](#)]
16. Yao, P.; Wang, W.; Huang, C.Z.; Wang, J.; Zhu, H.T.; Kuriyagawa, T. Indentation Crack Initiation and Ductile to Brittle Transition Behavior of Fused Silica. *Adv. Mater. Res.* **2013**, *797*, 667–672. [[CrossRef](#)]
17. Imanakam, O. Lapping mechanics of glass-especially on roughness of lapped surface. *Ann. CIRP* **1966**, *23*, 227–233.
18. Lambropoulos, J.; Jacobs, S.D.; Ruckman, J. Material removal mechanisms from grinding to polishing. *Ceram. Trans.* **1999**, *102*, 113–128.
19. Buijs, M.; Korpel-van Houten, K. A model for lapping of glass. *J. Mater. Sci.* **1993**, *28*, 3014–3020. [[CrossRef](#)]
20. Bulsara, V.H.; Ahn, Y.; Chandrasekar, S.; Farris, T.N. Mechanics of polishing. *J. Appl. Mech.* **1998**, *65*, 410–416. [[CrossRef](#)]
21. Evans, C.J.; Paul, E.; Dornfeld, D.; Lucca, D.A.; Byrne, G.; Tricard, M.; Klocke, F.; Dambon, O.; Mullany, B.A. Material removal mechanisms in lapping and polishing. *CIRP Ann.* **2003**, *52*, 611–633. [[CrossRef](#)]

